Surface Potential Solution for a nanoscale Double Gate MOSFET

Meenakshi Gupta
Department of Electronics & Communication Engineering
Manav Rachna University

ABSTRACT

Power consumption is a major concern for many applications such as mobile phones and medical devices. In these applications, power consumption is often a more important issue than speed. Reduction in Power consumption is possible by operating a circuit in the subthreshold regime. Thus Double-gate (DG) devices are being considered a very promising candidate for such applications [2]. Compact models are at the heart of CAD tools, and thus, accurate analytical models for MOS devices may be the major concern in future IC technology. Many 2-D models for the electrostatics and the drain current in short-channel DG MOSFETs were presented earlier [3]–[7].A physics-based model, which includes both the inter-electrode capacitive coupling and the effects of the inversion charge, covers a wide range of bias conditions. However, to achieve self-consistency, iterations are required. This modeling based on conformal mapping techniques gives a unified potential solution for a wide range of channel lengths, including ultrashort devices. Here, in this paper conformal mapping approach is combined with parabolic approximations to derive an explicit compact drain–current model for the subthreshold regime.

Keywords: DG-MOSFET, gate oxide thickness, Schottky contacts, DIBL etc.

INTRODUCTION

In this work the proposed model (see Fig. 1) has a gate length of $L = 25$ nm, a silicon thickness of $t_{si} = 12$ nm, a p-type body doping of $N_a = 10^{15}$ cm-3, and a high-_ gate insulator with a relative permittivity of $\_ox = 7$ and a thickness of $t_{ox} = 1.6$ nm. To simplify the calculations, we replace the insulator thickness t_{ox} by an electrostatically equivalent silicon layer of thickness $t'_{ox} = t_{ox}\_si/\_ox$, where $\_si = 11.8$ is the relative permittivity of silicon.
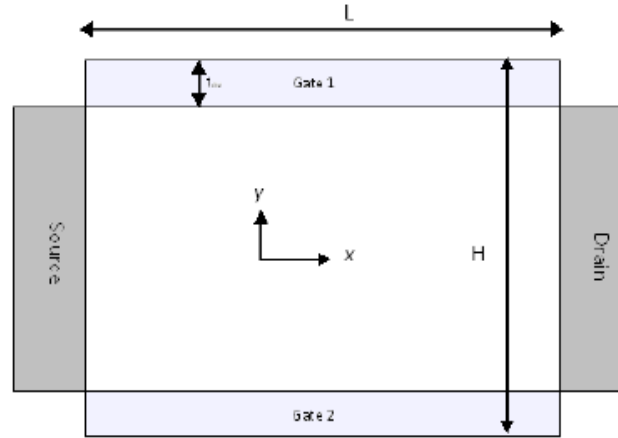
Fig. 1. Schematic cross section of the DG MOSFET.

Hence, the thickness of the extended body becomes $H = t\text{si} + 2t'\text{ox}$. As gate material, we select a near-midgap metal with a work function of 4.53 eV. Idealized Schottky contacts with a work function of 4.17 eV (corresponding to that of n+ silicon) are assumed for the source and drain. The aforementioned device dimensions are such that a classical treatment of the electron distribution in the device body is justified [10], [11]. Although the drain current has a significant quasiballistic component in the present device, we have shown that using a drift-diffusion transport mechanism with constant mobility agrees very well with simulated drain currents using more advanced transport formalisms [7]. For the device dimensions considered, the doping density of the device body has negligible influence on the body electrostatics for $Na < 1017$ cm−3.

DRAIN–CURRENT MODELING
In the subthreshold regime, the electrostatics in the device body is dominated by the interelectrode capacitive coupling between electrodes. This can be described by a 2-D Laplace equation using the potentials of the electrodes as boundary conditions. Small correction terms can be added to account for the finite oxide gaps in the four corners of the boundary [6]. An analytical solution of the potential distribution in the extended body is obtained by first performing a conformal mapping of the device cross section from the normal (x, y) plane to the upper half-plane of the complex (u, iv) plane defined by the appropriate Schwartz–Christoffel transformation and then using parabolic approximations to get simple analytical solutions in the (x, y) plane. The transformation is given as [3], [7].

$$z = x + iy = \frac{L}{2} \frac{F(k, w)}{K(k)} \tag{1}$$

where $F(k,w)$ is the complex elliptic integral of the first kind, $K(k) = F(k, 1)$ is the corresponding complete elliptic integral, and $w = u + iv$. The modulus k is a constant between 0 and 1, which is determined by the

geometric ratio *L/H* [3], [7]. The drain current based on drift-diffusion theory can be expressed as

$$I_d = -q\mu_n W \iint n(x,y) \frac{dV_F(x)}{dx}\, dy dx \tag{2}$$

where the double integral runs over the entire silicon body. Here, *W* is the device width, μ*n* is the electron mobility, *n(x, y)* is the electron distribution, and *VF* (*x*) is the quasi- Fermi potential, which is assumed to be constant over any given cross section perpendicular to the *x*-axis. Invoking current continuity along the channel and separating (2) into coordinate-dependent and *VF* dependent parts, we obtain

$$I_d = \frac{W q \frac{n_i^2}{N_a} \mu_n V_{th} \left[1 - exp\left(-\frac{V_{ds}}{V_{th}}\right)\right]}{\int_{-L/2}^{L/2} \frac{dx}{\int_{t'_{ox}}^{t_{si}+t'_{ox}} exp\left[\frac{\varphi(x,y)}{V_{th}}\right] dy}} \tag{3}$$

Here, *V*th is the thermal voltage, *ni* is the intrinsic carrier concentration in silicon, *Vds* is the drain–source voltage, and _(*x, y*) is the potential distribution of the extended body (including the effective silicon thicknesses *t'*ox) determined from the interelectrode coupling [4], [6]. The integrals in (3) do not have simple analytical solutions because of the functional form of _(*x,y*). Instead, we define an effective silicon thickness *tsie*(*x*) over which _(*x, y*) can be taken as constant in *y* and equal to its value _(*x,H/2*) at the source-to-drain (S-D) symmetry line, thereby accounting for the total number of electrons in each cross section. A parabolic potential distribution in the *y*-direction has been shown to be a good approximation in subthreshold [6], i.e.,

$$\varphi(x,y) \approx \varphi_c(x)\left[1 - \left(1 - \frac{2y}{H}\right)^2\right] + V_{gs} - V_{FB} \tag{4}$$

where _*c*(*x*) = _(*x,H/2*) − *Vgs* + *VFB* is the difference between the potential at position *x* on the S-D symmetry line and that of the gate-silicon interface of the extended body, *Vgs* is the gate-source potential, and *VFB* is the flatband voltage of the gate. We note that a slight error of the potential in the oxide regions, due to the deviation from a linear behavior in (4), does not translate into a significant error in the silicon region, which is important for modeling the drain current. Moreover, the inaccuracy is lessened by operating with the equivalent silicon thickness *t'*ox instead of the real oxide thickness *t*ox. Furthermore, in subthreshold, the body potential in any cross section perpendicular to the *x*-axis has its maximum at the S-D symmetry line. Hence, the current density is highest along this line.Using (4) together with Boltzmann statistics for the electron distribution, *tsie*(*x*) can be expressed as follows by equating the charge sheet density in a rectangular well of thickness *tsie*(*x*) with the parabolic well of thickness *t*si, i.e.,

$$t_{sie}(x) = \int_{t'_{ox}}^{t'_{ox}+t_{si}} exp\left[-\frac{\varphi_c(x)}{V_{th}}\left(1 - \frac{2y}{H}\right)^2\right] dy \tag{5}$$

The integral in (5) has an analytical solution in terms of error functions. However, further simplifications are needed in order to obtain an analytical solution for the integral over x in (3). The first step is to calculate the value $t_{sim} = t_{sie}(x_m)$ at the position x_m of the barrier maximum using (5) and then approximate $1/t_{sie}(x)$ by a parabolic function on either side of the maximum, requiring that $t_{sie} = t_{s,d}$ at the source and drain, i.e.,

$$\frac{1}{t_{sie}(x)} \approx \frac{1}{t_{sim}} + \left(\frac{1}{t_{s,d}} - \frac{1}{t_{sim}}\right)\left(\frac{x_m - x}{x_m \pm \frac{L}{2}}\right)^2 \qquad (6)$$

The upper and lower signs in front of $L/2$ apply for $x < x_m$ (source side) and $x > x_m$ (drain side), respectively. The barrier maximum is determined from the following analytical expression for the interelectrode potential distribution along the S-D symmetry line in the (u, iv) plane where

$$v = \sqrt{k^{-1} - u^2} \quad \text{[6], [7]:}$$

$$\begin{aligned}
\varphi(u) = V_{gs} - V_{FB} - \frac{1}{\pi} \times \Bigg\{ &(V_{gs} - V_{FB} - V_{bi})\left[\tan^{-1}\left(\frac{1-ku}{\sqrt{k-k^2u^2}}\right) - \tan^{-1}\left(\frac{k(1-u)}{\sqrt{k-k^2u^2}}\right)\right] \\
&+ (V_{gs} - V_{FB} - V_{bi} - V_{ds})\left[\tan^{-1}\left(\frac{1+ku}{\sqrt{k-k^2u^2}}\right) - \tan^{-1}\left(\frac{k(1+u)}{\sqrt{k-k^2u^2}}\right)\right] \Bigg\}
\end{aligned}$$

(7)

Differentiating (7) with respect to u, we find the following expression for the position of the barrier maximum:

$$u_m = -\frac{(1+k)V_{ds}}{2k(2V_{bi} + V_{ds} - 2V_{gs} + 2V_{FB})} \qquad (8)$$

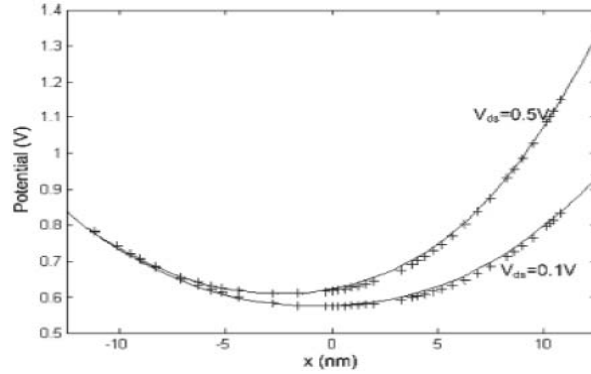$$u_m = \sqrt{\frac{1}{k} - u^2_m}$$

Fig. 2. Comparison of the modeled and (solid curves) numerically simulated potential variation along the S-D symmetry line for $V_{gs} = V_{FB} = -0.48$ V and $V_{ds} = 0.1$ and 0.5 V.

Using the inverse mapping function of (1), given in terms of the Jacobian elliptic functions [5], we obtain a precise value of the position x_m. The corresponding potential is $\varphi_m = \varphi(x_m, H/2) = \varphi(u_m)$, which is obtained directly from (7) using (8). The aforementioned analysis slightly overestimates the potential in the channel and,

thus, also overestimates the current. This occurs due to the fact that, near the source and drain contacts, the potential is relatively large, allowing a significant amount of electrons to accumulate. Thus, it is necessary to consider their electrostatic effect even under subthreshold conditions. This effect is included simply by adjusting the boundary conditions at the source and drain,
respectively, as follows [6], [7]:

$$V_{cs} = V_{bi} - \frac{V_{th}}{2}\left(\frac{E_\circ}{E_s}\right)^2$$

$$V_{cd} = V_{bi} + V_{ds} - \frac{V_{th}}{2}\left(\frac{E_\circ}{E_d}\right)^2 \tag{9}$$

Es and *Ed* represent total surface electric fields at the source and drain contacts [6], c th s φ2qN V /φo E , and *Nc* is the doping density at these contacts. The next step in solving the remaining integral over *x* in (3) is to find a simplified approximation of φ(*x,H/2*)) in the (*x, y*) plane. For this, we again resort to parabolic functions and write similar to (6)

$$\varphi(x, H/2) \approx \varphi_m + (\varphi_{s/d} - \varphi_m)\left(\frac{x_m - x}{x_m \pm L/2}\right)^2 \tag{10}$$

where, for the source side of the barrier, we use φ*s/d* = φ*s* = φ(−*L/2,H/2*) = *V*cs together with the + sign in front of *L/2*, and for the drain side, we use φ*s/d* = φ*d* = _(*L/2,H/2*) =*V*cd together with the − sign in front of *L/2*.

CONCLUSION

This developed accurate compact subthreshold model for DG MOSFETs is based on the use of precise conformal mapping techniques in combination with parabolic approximations for evaluating the body electrostatics. This model is physics-based and includes no fitting parameter. Potential graph shows good agreement with the numerical simulation from ATLAS.

REFERENCES

[1] X. Liang and Y. Taur, "2-D analytical solution for SCEs in DG MOSFETs," *IEEE Trans. Electron Devices*, vol. 51, no. 9, pp. 1385– 1391, Sep. 2004.
[2] S. K. Vishvakarma, A. K. Saxena, and S. Dasgupta, "Two dimensional analytical potential modeling of nanoscale fully depleted metal gate double gate MOSFET," *J. Nanoelectronics Optoelectronics*, vol. 3, no. 3, pp. 297–306, Dec. 2008.
[3] Y. Omura and K. Izumi, "Quantum mechanical influences on shortchannel effects in ultra-thin MOSFET/SIMOX devices," *IEEE Electron Device Lett.*, vol. 17, no. 6, pp. 300– 302, Jun. 1996.

[4]   H.-S. P.Wong, D. J. Frank, and P.M. Solomon, "Device design for doublegate, ground-plane, and single-gated ultra-thin SOI MOSFETs at the 25 nm channel length generation," in *IEDM Tech. Dig.*, Dec. 1998, pp. 407–410.

[5]   E. Weber, *Electromagnetic Fields*, vol. 1. New York: Wiley, 1950.

[6]   T. A. Fjeldly and M. S. Shur, "Threshold voltage modeling and the subthreshold regime of operation of short-channel MOSFETs," *IEEE Trans. Electron Devices*, vol. 40, no. 1, pp. 137–145, Jan. 1993.

[7]   H. Børli, S. Kolberg, and T. A. Fjeldly, "Physics based current and capacitance modeling of short-channel double-gate and gate-all-around MOSFETs," in *Proc. 2ⁿᵈ IEEE INEC*, Shanghai,China,Mar.2. , pp. 844–849.